Analysis of the intrinsic magnetic properties of R_2Fe_{17} single crystals (R=Y, Dy, Ho, Er)

B. García-Landa,* P. A. Algarabel, and M. R. Ibarra
Departamento de Física de la Materia Condensada e Instituto de Ciencia de Materiales de Aragón, Facultad de Ciencias, Universidad de Zaragoza-CSIC, 5009-Zaragoza, Spain

F. E. Kayzel and J. J. M. Franse
Van der Waals-Zeeman Laboratorium, University of Amsterdam, Amsterdam, The Netherlands
(Received 9 September 1996; revised manuscript received 9 December 1996)

The magnetic behavior of some R_2Fe_{17} single crystals have been analyzed quantitatively in a wide temperature range, using a two-sublattice approximation for the magnetic structure and taking into account isotropic exchange and single-ion crystal-field interactions. The $3d$ sublattice behavior has been described phenomenologically, from the study of the experimental magnetization results in a Y_2Fe_{17} single crystal. The parameters A_2^0, A_4^0, A_6^0, A_6^6, describing the crystal-field interaction in the different R_2Fe_{17} compounds (R=Er, Dy, Ho) have been determined. The calculated magnetic behavior shows good agreement with experimental magnetization results in the temperature range 4.2 to 300 K, demonstrating the reliability of the determined parameters. [S0163-1829(97)05813-X]

I. INTRODUCTION

In the search for less expensive new permanent magnet materials, interest has been focused in recent years on the iron-rich rare-earth (R) intermetallic compounds. Some examples are the ternary compounds $R_2Fe_{14}B$ and the isomorphous $R_2Fe_{14}C$, the materials characterized by the formula $RFe_{12-x}T_x$, where T=Al, Ti, V, Cr, Mo, W, and Si, the ternaries $R_2Fe_{17}C_x$, $R_2Fe_{17}N_x$, and R_6Fe_{23}. In particular, materials obtained by nitrogen insertion in the 2:17 matrix have shown promising properties for permanent magnet applications, comparable with those of $Nd_2Fe_{14}B$.[1] Knowing the intrinsic magnetic properties of the R_2Fe_{17} family is the first step for understanding the basic magnetic properties of the ternary interstitial compounds derived from them.

Several attempts have been made up to now in order to explain the magnetic properties of these intermetallics from a microscopic point of view. Of particular interest is the knowledge of the anisotropy arising on the rare-earth sublattice, originated in the crystal electric-field (CEF) interaction. This interaction can be fully described by the so-called CEF parameters A_n^m, which account for the intensity of such interaction. The CEF parameter set can be determined by means of fitting to the CEF-model different experimental results, such as magnetization measurements and inelastic neutron scattering. Examples of crystal-field analysis of the experimental behavior can be found for $R_2Fe_{14}B$,[2] $Dy(Fe_{14}Ti)$,[3] and also for the R_2Fe_{17} family.[4–7] For this last series the A_n^m values proposed in literature present a very strong dispersion, and we can say that the problem is still waiting for a more reliable solution. Different reasons can lead to this uncertainty not only in the precise values but also in the order of magnitude of the parameters. In the work of Ref. 5, based on an analysis of inelastic neutron-scattering experiments on Ho_2Fe_{17}, the A_n^m values deduced were derived in combination with an unrealistically small value of the molecular field.[8] For the works based on an analysis of the magnetic behavior, CEF parameters are given which give a good fit to the low-temperature isotherms (usually 4.2 K), but do not account for the magnetic behavior at higher temperatures.

This work attempts to provide more conclusive results on the CEF interaction in the R_2Fe_{17} compounds. For that purpose, in a previous paper,[9] the magnetization behavior of some R_2Fe_{17} compounds was investigated in a wide temperature range (from 1.5 to 300 K) using single-crystalline samples. Continuing in this line, an effort has been made to obtain a set of CEF parameters that explains the magnetic behavior in this wide temperature range. The CEF parameters that will be presented here have been obtained from the analysis of the magnetization isotherms at several temperatures, with the magnetic field applied along the different crystallographic directions. Although the R_2Fe_{17} structure presents two crystallographically distinct sites for heavy rare earths, we will assume in our treatment that the CEF anisotropy can be described using a single set of parameters averaged over the two sites. This approach, which reduces the number of parameters to half, has also been applied in previous works.[4–7] Arguments will be given later that can justify the use of this simplifying assumption for the R_2Fe_{17} series. In this study we show that the low-temperature magnetization analysis cannot by itself lead to conclusive results on the basis of the CEF model.

In the present work the four-dimensional CEF-parameter space is analyzed in detail. Several thousands of parameter sets are examined. The $\{A_n^m\}$ set is chosen randomly within a certain range in the parameter space. Assuming that this set describes the CEF interaction of the compound, we can calculate the magnetization behavior and compare it with the observed experimental one. In this way the set can be accepted or rejected as possible solution. The base of the procedure that we have followed in this work is similar to the one described in the paper of Ref. 10, applied to obtain the CEF parameters in the R_2Zn_{17} compounds from inelastic neutron-scattering measurements.

The process of determination of the CEF parameters from

the magnetization results is made step by step. First we consider an experimental magnetic isotherm obtained at temperature T_1, $M_{\rm exp}(T_1)$. Given a certain parameter set, if the calculated magnetization $M_{\rm cal}(T_1)$ lies for all the field range within the experimental error bar $M_{\rm exp}\pm\Delta M_{\rm exp}$, then the set is considered for further analysis. In this way we obtain several $\{A_n^m\}$ sets associated with the temperature T_1. In the following steps the number of possible solutions is reduced gradually by means of imposing the restrictions given by other measured isotherms $M_{\rm exp}(T_2)$, $M_{\rm exp}(T_3)$, etc. If adding more experimental restriction does not further reduce the number of CEF parameter sets, we have reached the limit of our experiment for determining the solution.

One of the problems we have to face is the fact that the computer calculation of the magnetization is highly time consuming. For this reason we have to reduce as much as possible the number of $(\mu_0 H_{\rm exp}, M_{\rm exp})$ points (magnetization at a certain magnetic field value $\mu_0 H_{\rm exp}$) to be calculated for each studied isotherm. A careful selection of the minimum number of these points must be done, in order to determine which CEF parameter sets are giving a good M fit in all the field range with a small waste of time. This choice has no rule, and depends on the particular features of the measured isotherms. For example, in Er_2Fe_{17} a first-order magnetization process (FOMP) takes place at low temperatures. In this case the experimental values corresponding to the magnetization and magnetic field just before and after the transition must be taken into account.

II. EXPERIMENT

All the experimental magnetization data considered in this work have been obtained from measurements on single-crystalline samples grown in the Van der Waals-Zeeman Institute, using the Czochralski technique. The magnetization measurements were performed on oriented single crystals of Y_2Fe_{17}, Er_2Fe_{17}, and Ho_2Fe_{17}. Different isotherms were measured at temperatures ranging between 1.5 and 300 K, each 50 K approximately (20 K interval for Er_2Fe_{17} compound at low temperatures). A sensitive vibrating sample magnetometer was used in steady magnetic fields up to 12 T. Details about the experimental results have been presented in the work given in Ref. 9. The high-field magnetization results (up to 35 and 51 T) as well as the experimental results on Dy_2Fe_{17} have been taken from literature (the references are given below).

III. THEORETICAL BACKGROUND

In the R-M compounds, where M is a $3d$ transition metal, the magnetization behavior is given by the interplay of two main contributions: the one arising from the localized R moments, and the one arising from the itinerant M moment. The first contribution is analyzed within the frame of the CEF model, as will be shown later. The determination of the $3d$ magnetic contribution from a theoretical point of view requires the use of complicated calculation formalisms, which is beyond the scope of this paper. We can introduce this contribution in a phenomenological and reliable way by taking into account the following considerations:

(i) Of the three magnetic interactions taking place in the R-M system, the direct $3d$-$3d$ exchange is much stronger than the $3d$-$4f$ coupling between the R and M moment, and the relatively weak $4f$-$4f$ indirect exchange between the localized rare-earth moments can be neglected. In such a system we can consider that the molecular field acting on the $3d$ moments is mainly determined by the $3d$-$3d$ exchange interaction which is the largest contribution to the free energy determining the magnetic ordering temperatures, as observed experimentally. The iron magnetic moments are ferromagnetically coupled below T_c, and couple antiferromagnetically to the magnetic moment of the heavy rare earths.

(ii) The electronic structure around the Fermi level is not expected to differ significantly from the one of the corresponding yttrium compound with the same stoichiometry. For these reasons we can assume that the magnetic behavior of the $3d$ sublattice in R_2Fe_{17} is similar to that presented by the nonmagnetic ''rare-earth''-based compound, Y_2Fe_{17}. A study of the magnetization behavior on this intermetallic has been performed in order to obtain the phenomenological description of the $3d$-sublattice magnetization.

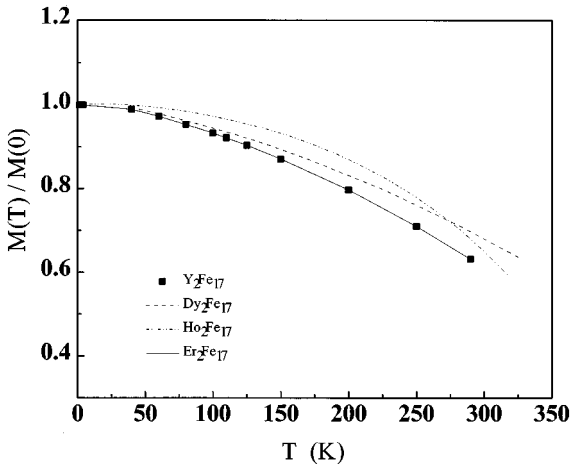

FIG. 1. Symbols: determined thermal dependence of the spontaneous magnetization in Y_2Fe_{17}. Lines: thermal dependence used for the indicated R_2Fe_{17} compounds.

A. Y_2Fe_{17}: The magnetic contribution of the $3d$ sublattice

One of the difficulties that we have to face in the analysis of the iron-based intermetallics is the large thermal variation of the magnetic properties of the $3d$ sublattice in the range 5–300 K. In order to give a full description of the behavior of this sublattice we have to know the spontaneous magnetization at each temperature, $\mathbf{M}_{\rm Fe}(T)$, as well as the magnetic anisotropy. The last can be described phenomenologically by means of the anisotropy constants K_1 and K_2, which are also temperature dependent.

The spontaneous magnetization of the iron sublattice at different temperatures was obtained from the magnetization isotherms of the single crystal Y_2Fe_{17}. The resulting thermal variation is shown in Fig. 1. When considering the thermal variation of the iron sublattice in an R-based compound we have to take into account the deviation of the value of the ordering temperature with respect to the T_c value of Y_2Fe_{17}. The ytrium-based compound has an ordering temperature of 327 K.[4] In this way, the Curie temperature is very close for

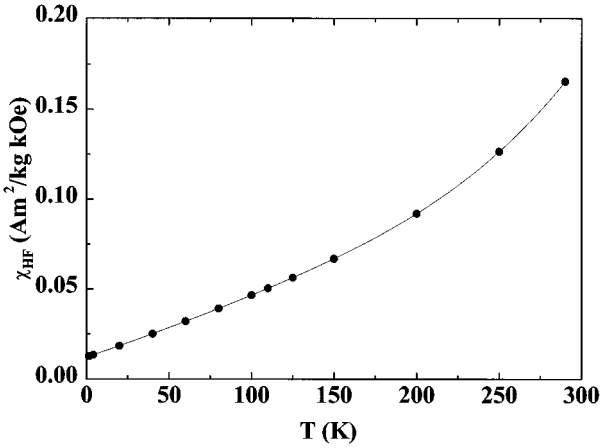

FIG. 2. Thermal variation of the high-field susceptibility of Y_2Fe_{17}.

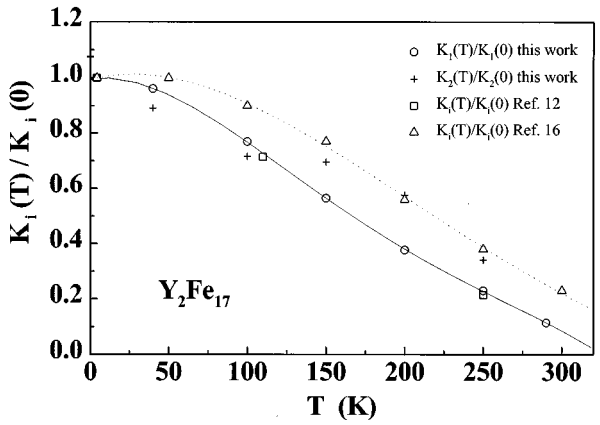

FIG. 3. Thermal variation of the anisotropy constants in Y_2Fe_{17}, obtained according to the Sucksmith-Thompson relation: open circles K_1, crosses K_2. The results from other authors have also been represented: squares (Ref. 12), triangles (Ref. 16). The lines are guides to the eye.

Er_2Fe_{17} (310 K) (Ref. 4), and Ho_2Fe_{17} (335 K),[11] but an important difference exists in the case of Dy_2Fe_{17} compound (370 K).[4] In the last case a renormalization of the temperature scale has been made for calculating the thermal variation of the magnetization of the $3d$ sublattice. The result is shown in the same figure. The scaled magnetization thermal dependence could not successfully explain Ho_2Fe_{17} magnetic behavior for high temperatures, and the curve displayed in the figure was determined for this compound, as will be explained later.

As observed in Y_2Fe_{17}, we have to consider the nonnegligible anisotropy in the module of the $3d$ magnetization,[12,13] which can be expressed in the following manner:

$$M_{\mathrm{Fe}}(\theta,T)=M_{\mathrm{Fe}}(T)[1-p\ \cos^2\theta], \tag{1}$$

where θ is the angle between the iron sublattice magnetization and the **c** axis and $p=0.02$.[12]

In a detailed description of the $3d$ sublattice the nonnegligible high-field susceptibility χ_{Hf} must also be considered. In fact, the existence of this susceptibility is responsible for the observed modification of the $3d$ spontaneous magnetization in the R-M compound, vs the value obtained in the Y-M compound. The $3d$ magnetization in the R-M system has a higher value (about 3% more) due to the effect of the molecular field produced by the presence of a magnetic moment at the R site on the $3d$ moment. The strong variation with temperature of χ_{Hf} in Y_2Fe_{17} is shown in Fig. 2.

After correcting for the demagnetizing field, the anisotropy constants K_1 and K_2 were determined by the Sucksmith-Thompson relation.[14] For an easy-plane system this relation becomes[15]

$$H/M_c=-2(K_1+4K_2)/M_s^2+(4K_2/M_s^4)M_c^2 \tag{2}$$

(M_s is the spontaneous magnetization, M_c the magnetization measured along the hard-**c** direction). The values for the anisotropy constants at 4.2 K according to our results are $K_1=-50.4$ K/f.u. and $K_2=-0.85$ K/f.u. The first, K_1, is a 13% smaller than in the previous work of Ref. 12. This difference is revealing the large effect of nonstoichiometry[16–18] on the anisotropy constants. In the work of Ref. 16, a value of -48.5 K/f.u. is obtained for K_1 when considering the ideal stoichiometry, whereas -43.8 K/f.u. is concluded when the real stoichiometry of the compound is taken into account. To the same reason can be attributed the deviations in the second-order anisotropy constant K_2, whose value at 4.2 K has been reported to be $+4.7$ K/f.u.[12] The thermal dependence used in our calculations has been obtained using the Sucksmith-Thompson relation for the measured isotherms and is shown in Fig. 3. We have also compared in this figure the results obtained by other authors. The thermal variation of the anisotropy constants is in good agreement with the results of the above-mentioned work.

As was noted for the thermal dependence of the $3d$ sublattice magnetization, a renormalization in the temperature scale has been performed for calculating the thermal dependence of K_1 for the R_2Fe_{17} compounds, according to the exact value of T_c.

B. Determination of the equilibrium magnetization: Formulation

The Hamiltonian of a rare-earth ion in the R-M intermetallics involves three main contributions: the electrostatic CEF interaction, the Zeeman term and the $3d$-$4f$ exchange term. The last one can be expressed in a mean-field approximation by means of an effective exchange field, $\mathbf{H}_{\mathrm{ex}}$, acting on the magnetic moment of R:

$$H_R=H_{\mathrm{CEF}}+g_J\mu_B\mathbf{J}\cdot\mathbf{H}_{\mathrm{eff}}+2(g_J-1)\mu_B\mathbf{J}\cdot\mathbf{H}_{\mathrm{ex}}. \tag{3}$$

$\mathbf{H}_{\mathrm{eff}}$ is the internal effective magnetic field acting on the ion, H_{CEF} represents the CEF Hamiltonian for hexagonal symmetry and g_J is the Landé g factor. In this expression we have considered that $\mathbf{H}_{\mathrm{ex}}$ is proportional and antiparallel to the iron sublattice magnetization, $\mathbf{M}_{\mathrm{Fe}}(T)$. The value of the exchange interaction existing between the $4f$ and $3d$ sublattices has been taken from literature, determined from high-field magnetization studies.[8]

The R_2Fe_{17} compounds with a heavy rare earth present a hexagonal structure of the type Th_2Ni_{17}, with space group $P6_3/mmc$.[19] The R ion occupies two crystallographic different sites, $2b$ and $2d$, both with the same point symmetry

TABLE I. CEF parameters A_n^m (in units of Ka_0^{-n}) for R_2Fe_{17}.

R	A_2^0	A_4^0	A_6^0	A_6^6	Reference
R	−420				PCM in R_2Co_{17} site b (Ref. 21)
	+310				PCM in R_2Co_{17} site d (Ref. 21)
	−532				PCM in R_2NI_{17} site b (Ref. 22)
	+222				PCM in R_2Ni_{17} site d (Ref. 22)
	−150	−0.05	−0.006		PCM in R_2Fe_{17} (Ref. 4)
Dy	−36.06	−9.49	+0.046	−21.88	(this work)
	−0.97	−4.6	+0.06		4
Ho	−88.42	−9.78	−0.28	−4.07	(this work)
	−900	−30.3	−3.4	−1.7	5
Er	−24.58	−11.88	+0.4915	−13.59	(this work)
	+17.9	−8.9			4
	−202.7	−13.3		−95.5	6
	−56.3	−14.4		−39.4	7
Tb	+5.3	−0.24	−7.8		4

$(-6m2)$. These sites present a similar surrounding with respect to the transition-metal atoms but a dissimilar surrounding regarding the other rare-earth atoms. The CEF Hamiltonian associated with this point symmetry is expressed in the Stevens formulation[20] as

$$H_{\mathrm{CEF}}=B_2^0O_2^0+B_4^0O_4^0+B_6^0O_6^0+B_6^6O_6^6, \tag{4}$$

where $B_n^m=\theta_m\langle r^m\rangle A_n^m$, and where θ_m represents the Stevens coefficients (α_J, β_J, and γ_J for $m=2$, 4, and 6, respectively), $\langle r^m\rangle$ are the Hartree-Fock radial integrals, and A_n^m are the CEF parameters. The value of the A_2^0 parameter has been calculated using the point-charge model (PCM) for the two sites in the Th_2Ni_{17} structure[21] for the R_2Co_{17} compounds and also for the R_2Ni_{17} compounds[22] (see Table I). After the PCM calculation the values at each R site have different signs, indicating the possibility of competitive contribution to the magnetocrystalline anisotropy from these sites. Experimentally the possibility of a difference between the CEF interaction in both sites in the hexagonal structure is not completely clear. While the Mössbauer spectra of Tm_2Fe_{17} and Tm_2Co_{17} were successfully interpreted in terms of two subspectra in an unambiguous way,[23] no difference between sites was found in Mössbauer analysis of Tm_2Ni_{17}.[24] In addition, the anisotropy constants deduced[23] did not explain the observed magnetization results. No difference was observed by inelastic neutron-scattering experiments on the compound Ho_2Co_{17},[5] where the lower part of the low-energy level schemes was observed to be practically the same for both sites.

A small or negligible difference in the crystal-field interaction experienced by the $4f$ electrons (and hence A_2^0) at each site would not be surprising if we consider that this interaction is mostly determined by the rare-earth valence electrons ($5d$ and $6p$).[25] In our approach we assume that the magnetic behavior of the rare-earth sublattice can be fully described by a set of four CEF parameters averaged over the two sites. This approximation in the description of the magnetic behavior of the system is reasonable if we take into account that the rare-earth sites are strongly coupled to the iron sublattice, whereas the $4f$-$4f$ interaction is negligible.

The equilibrium magnetic configuration of the system is determined by the following procedure: for a given field $\mathbf{H}_{\mathrm{eff}}$ and a direction of the iron sublattice magnetization given by the polar angles (θ,ϕ), we calculate the eigenvalues E_i and eigenvectors $|\Psi_i\rangle$ $(i=2J+1)$ by diagonalizing the rare-earth Hamiltonian H_R. The equilibrium direction (θ_0,ϕ_0) of the iron sublattice magnetization is obtained by minimizing the free energy of the system:

$$F(\theta,\phi)=-2k_BT\ \ln\ Z_R+K_1(T)\sin^2(\theta)+K_2(T)\sin^4(\theta) -\mathbf{M}_{\mathrm{Fe}}\cdot\mathbf{H}_{\mathrm{eff}}, \tag{5}$$

where $Z_R=\ln[\mathrm{Tr}(e^{-\beta H_R})]$ is the partition function of the R ion. The magnetic moment of the R_2Fe_{17} system results from the addition of the contribution arising from the iron and the rare-earth sublattices:

$$\mathbf{M}(T)=2\mathbf{M}_R(T)+\mathbf{M}_{\mathrm{Fe}}(T,\theta_0,\phi_0), \tag{6}$$

with

$$\mathbf{M}_R(T)=-\mu_Bg_J\sum_i\ \langle\Psi_i|J|\Psi_i\rangle e^{-\beta E_i}/Z_R. \tag{7}$$

Given a CEF parameter set, the equilibrium magnetization of the system is calculated in this way at a certain temperature and for different values of the applied magnetic field. We calculate the values $[\mu_0H_{\mathrm{cal,i}}(T),\ M_{\mathrm{cal,i}}(T)]$ that have to be compared with experiment in order to evaluate the considered parameter set (i indicating different experimental data obtained at different magnetic fields).

IV. RESULTS AND DISCUSSION

A. Er_2Fe_{17}

The magnetic behavior of this compound has very marked features that impose restrictive conditions for the CEF parameter search. A FOMP takes place in the low-temperature range ($T<125$ K approximately), for the field applied along the hard-c direction.[9] The parameters determined have to give also a quantitative explanation of the field-induced tran-

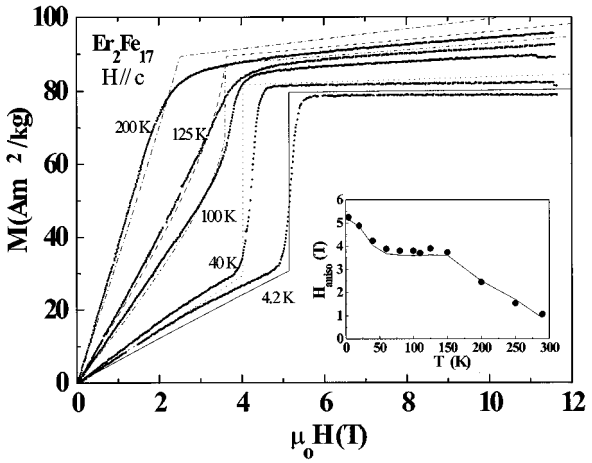

FIG. 4. Magnetization isotherms in Er_2Fe_{17} for the magnetic field applied along the hard-**c** magnetization direction at some selected temperatures: the dots correspond to the experimental results, the lines represent the calculation for the set of parameters determined in this work (see Table I). In the inserted figure the thermal evolution of the anisotropy field (critical field in the case $T<125$ K) has been represented. The solid circles correspond to the experimental data and the line represents the calculated behavior.

sitions observed at high values of the magnetic field, when the last is applied along the **a** and **b** directions.

The first step in the analysis of the magnetization of Er_2Fe_{17} has been to determine the CEF parameter sets giving a good fit of the 4.2 K experimental **c** isotherm for an applied field up to 12 T (see Fig. 4). A jump in the magnetization value takes place with increasing magnetic field: from 32.0 A m^2/kg at 50.2 kOe to 78.4 A m^2/kg at 53.8 kOe at 4.2 K. The different parameter sets giving a correct fit to this transition have been represented by dots in Figs. 5(a) and 5(b). These A_n^m parameters have been found in combination with a value of the exchange field $H_{ex}=127.5$ K.[12] Figure 5(a) corresponds to the projection of the $\{A_n^m\}$ four-dimensional solution on the A_2^0/A_4^0 plane, whereas Fig. 5(b) corresponds to the projection on the A_6^0/A_6^6 plane. This very wide region of the A_n^m space can be reduced consecutively if we add new restrictions: we impose the fit to the experimental magnetization isotherms measured at higher temperatures. A strong reduction on the allowed parameter region occurs when imposing the fit to the $T=40$ K isotherm and of the $T=80$ K isotherm. Selecting between the obtained solutions the parameter sets that give a good fit to the experimental isotherms at higher temperatures (up to 290 K) gives practically no reduction in the number of solutions found.

The search procedure described up to now will be referred in the following as the ''first step'' of the parameter search. In this first step we only made use of the measurements performed using magnetic fields up to 12 T applied along the hard-**c** direction. The resulting parameters are observed to give a good fit also to the **a** and **b** isotherms in the mentioned field range. In a second step we try to obtain more precise values of the parameters by introducing other available experimental conditions: the magnetic measurements performed with high magnetic fields (up to 51 T) applied along the **a** and **b** axis.[26] Two field-induced transitions are observed experimentally: at 38 T along the **a** axis and at 45 T along the **b** axis (see Fig. 6). As the single crystal used in

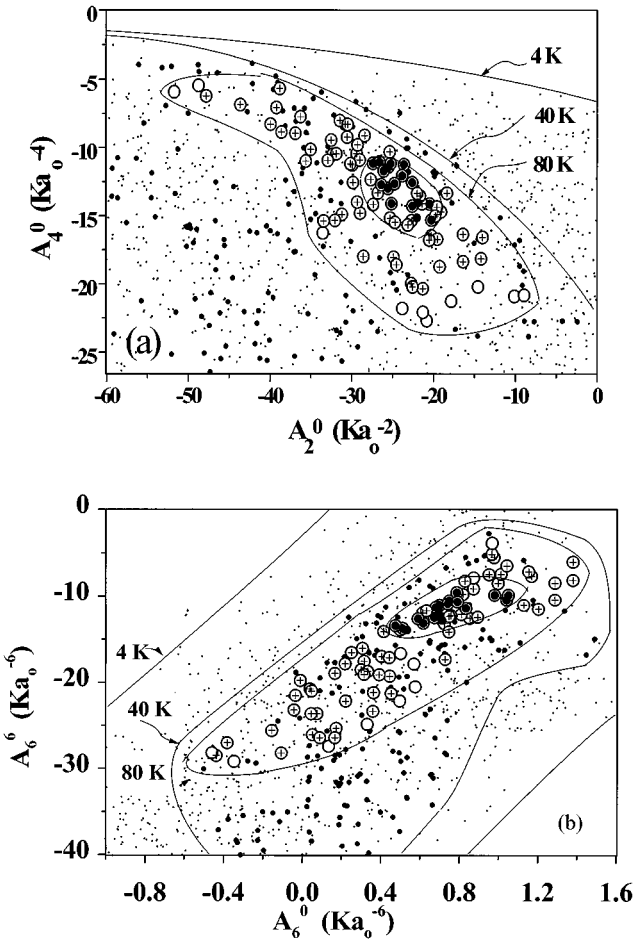

FIG. 5. Projection on the A_2^0/A_4^0 (a) and A_6^0/A_6^0 planes (b), of different $\{A_n^m\}$ parameter sets: the four-dimensional solutions fitting the $T=4.2$ K **c** isotherm of Er_2Fe_{17} are represented (dots), $T=40$ K (solid small circles), $T=80$ K (open circles), $T=100$ K (crosses) and the sets fitting also the high-field results (solid big circles). The solid lines are visual guides delimiting the region of the space where the solutions are found.

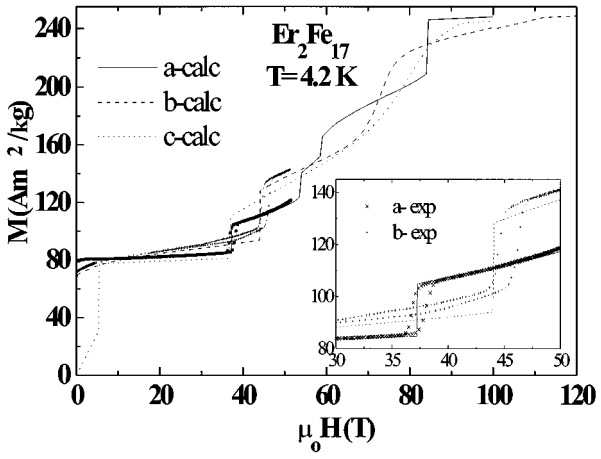

FIG. 6. Magnetization isotherms for the field applied along the directions **a** and **b** at 4.2 K for Er_2Fe_{17}. The symbols correspond to the experimental results (Ref. 26), the solid lines represent the calculation for the set of parameters determined in this work (see Table I).

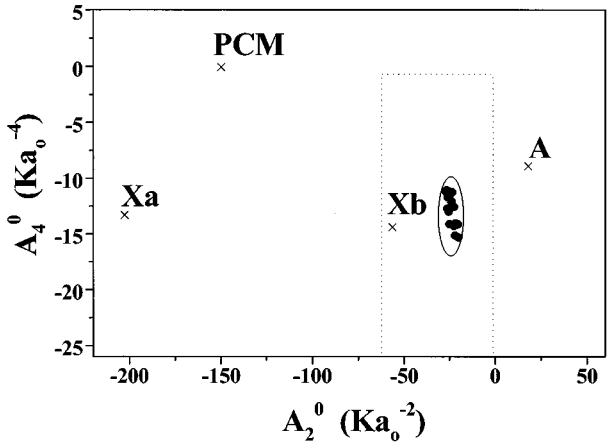

FIG. 7. Projection on the A_2^0/A_4^0 plane of the $\{A_n^m\}$ parameter sets for Er_2Fe_{17}: solutions determined in this work (solid circles), and solutions proposed by other authors: **Xa** (Ref. 6), **Xb** (Ref. 7), **PCM** indicates the solution according to point-charge model calculations (Ref. 4), **A** indicates the solution determined from fitting to experimental results in the work of Ref. 4.

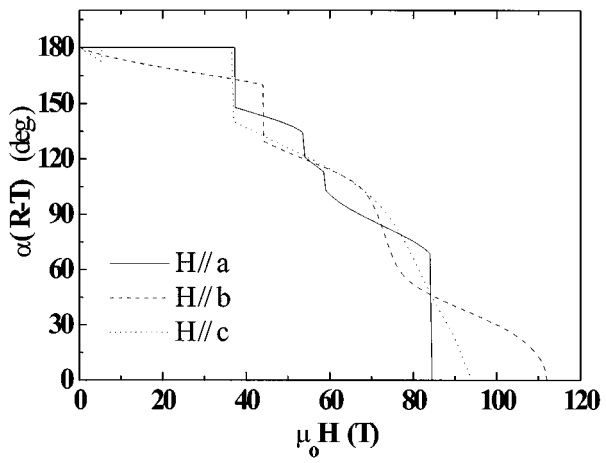

FIG. 8. Calculated field dependence of the angle $\alpha_{R\text{-}T}$ existing between the rare-earth and iron sublattices for different directions of the applied magnetic field.

these experiments was not the same used in our measurements, a correction of the value of the spontaneous magnetization has been done in the corresponding analysis. The parameters giving a good fit to our magnetization measurements (first step of the search) have been examined for these additional experimental restrictions. The solution is represented by the big solid circles in Figs. 5(a) and 5(b). The values of the parameters determined in this way have been compared with other values proposed by different authors in Fig. 7, where the same kind of projection as in Fig. 5(a) has been used.

We have selected, between the parameters given in Fig. 5, the set giving quantitatively the best fit to the experimental results. The A_n^m values are given in Table I. The calculated magnetization isotherms are compared with experimental results in Figs. 4 and 6. The field-induced transition occurring when the field is applied along the hard-**c** axis is present for temperatures lower than 125 K approximately. Under this temperature the free energy of the system as a function of θ presents two minima, separated by an energy barrier. When the value of the magnetic field increases, the system abruptly jumps from the high-angle minimum to a configuration parallel to the **c** axis. For temperatures close to 125 K the energy barrier between both minima becomes smaller and, at $T=125$ K, it has completely disappeared. In this situation the $3d$ sublattice magnetization is allowed to rotate continuously from the basal plane to the **c** axis with increasing field.

The prediction of the existence of the first field-induced transitions experimentally observed for the field applied along the **a** and **b** axis (see Fig. 6) is a common characteristic of all the parameters obtained on the first step of our search. Also the field position is quite independent on the selected set, but the same cannot be said for the predicted transitions occurring at higher fields. The existence of a transition at values of the field higher than 50 T for the **a** axis had already been noted by other authors,[7] but the field value given in that work is higher than the one determined from our calculations. One qualitative feature that has been taken into account in the second step of parameter selection leading to the solution set, is the fact that the magnetization isotherms along **a** and **b** for field values close to 50 T, present a nonlinear behavior (See Fig. 6). Before the transition the isotherm is slightly bent upwards. For the parameters that can explain this behavior three additional transitions are expected along the **a** direction at 4.2 K, at values of the field of 53.5, 58.5, and 84 T. A quick variation of the magnetization along the **b** axis occurs in the field range 66 to 81 T, but no sharp transition is observed. Also the calculations along the **c** direction have been represented in Fig. 6: a transition is predicted at 36.5 T, but no measurements are available up to now to confirm this result.

The field dependence of the angle $\alpha_{R\text{-}T}$, between the rare-earth and iron sublattice, has been represented in Fig. 8. When the rare-earth moment and iron magnetization are parallel the maximum magnetization value is reached. This happens at values of the magnetic field lower than 115 T for all the directions of the applied field. The relative position of the moment with respect to the [100], [010], and [001] directions is represented for some values of the field in Fig. 9. After these calculations, when the field is applied along **a**, the rare-earth and iron moments can present, for some values of the field, a component along the **c** direction. Also when the field is applied along the **c** direction the moments, initially along the [100] axis, can show a component along the **b** direction. After our calculations, the high-field transitions smoothen with temperature and for example, the anisotropy at 60 K becomes negligible for fields higher than 4.5 T.

The calculated results for the thermal variation of the magnetization with a field of 1 T applied along the easy magnetization direction have shown a good agreement in almost all the temperature ranges. The discrepancies occurring at high temperature can be due to the fact that the magnetization behavior of the $3d$ sublattice is not completely well described in this temperature range by the simple phenomenological analysis made in last section: at high temperatures the magnetization isotherms along the hard direction are not linear after reaching saturation.

B. Dy_2Fe_{17}

The experimental magnetization data of this compound have been taken from Ref. 12. In the mentioned work the

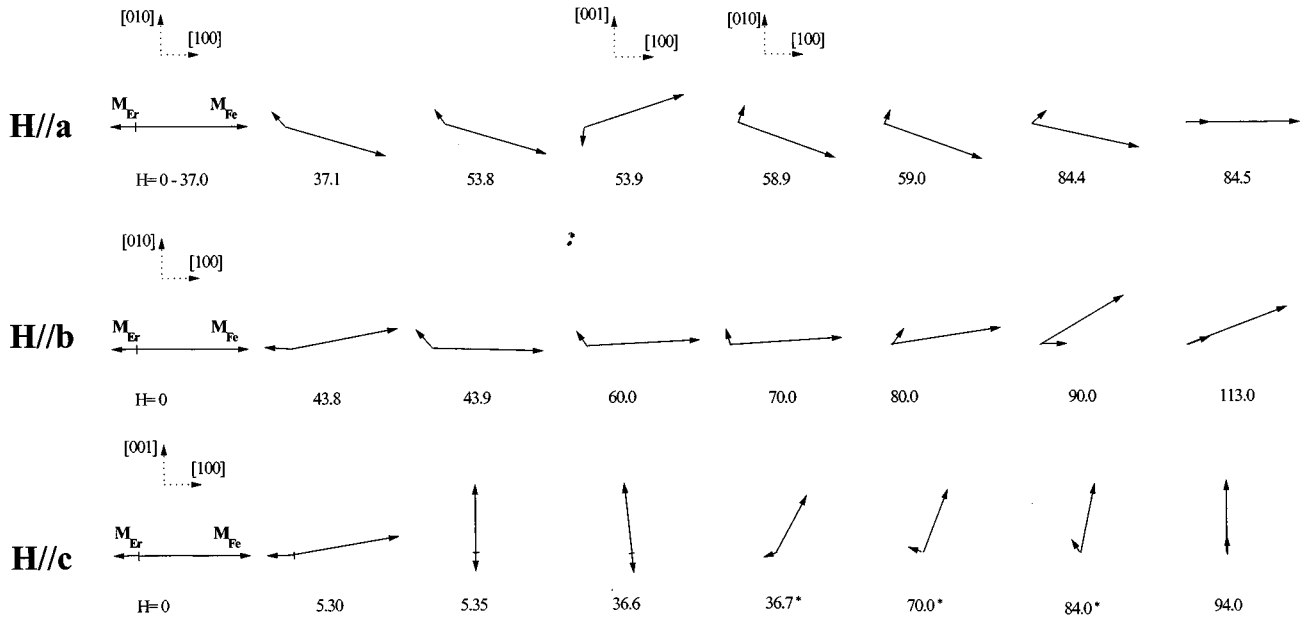

FIG. 9. Calculated spin structure of Er_2Fe_{17} at $T=4.2$ K for some values of the magnetic field (in tesla), applied along the **a** axis (upper figures), the **b** axis (middle figures), and **c** axis (lower figures). The configurations indicated with (∗) do not lay in the represented plane, but only these components of the moments are shown for simplicity.

$M(H)$ isotherms have been measured at 4.2 and 250 K, for the magnetic field applied along the three crystallographic directions. In our calculations the exchange field has been taken to be $H_{ex}=-143.0$ K.[27] Using the same parameters obtained as final solution for Er_2Fe_{17}, no satisfactory fit of the magnetization results is obtained for the dysprosium-based compound. In order to find the CEF parameters for this compound we have examined the A_n^m values obtained in the first step of the parameter search of the Er_2Fe_{17} compound. The initially wide parameter region to be tested is reduced considerably when imposing the fit to Dy_2Fe_{17} experimental data, as shown in Figs. 10(a) and 10(b). We can observe that the solution region for the last intermetallic is shifted with respect to the results for the erbium-based compound (contours represented by the solid lines in the same figure).

Between all the solution sets obtained, we have selected the parameters giving the best fit to the 4.2 K measurements, which are given in Table I. The magnetization isotherms calculated using these values is shown in Fig. 11, together with experimental data for the temperature 4.2 K. Field-induced transitions are expected to take place at 57.8 and 141.4 T for the easy-**a** axis, and at 70.6 T for the **b** axis. No sharp transitions are predicted along the hard-**c** direction, even for fields higher than 30 T. The two sublattices become parallel under application of magnetic fields in the order of 200 T. The resulting fit for the magnetization measurements at $T=250$ K is shown in Fig. 12 for the different directions of the applied field. The thermal variation of the magnetization with an applied field of 1 T along the different crystallographic directions is shown in the inset of Fig. 12. A good qualitative agreement is obtained. The anisotropy between the **a** and **b** axis for this value of the field disappears at about 160 K. The quantitative discrepancies observed can be attributed to deviations of the magnetization behavior of the $3d$ sublattice from the one observed in Y_2Fe_{17}.

C. Ho_2Fe_{17}

Although the parameters obtained scaling, those found for Er_2Fe_{17} give a quantitatively good explanation for the magnetization results observed at 4.2 K, discrepancies are found between the calculated and experimental thermal variation of the anisotropy field for which a faster reduction is predicted. The exchange field between the rare-earth and iron sublattice in the analysis has been taken to be $H_{ex}=-160$ K.[28,7]

The calculated results using the same values as determined for the Er_2Fe_{17} compound can be seen in Fig. 13 for $T=4.2$ K. As we observe when the magnetic field is applied along the hard-**c** direction, the magnetization already starts with a significant nonzero value, in contrast with our experimental observations. This is also the case for the rest of the solution parameter sets found for the erbium-based compound (solid circles in Fig. 5), with a spontaneous magnetization component along the **c** axis whose value can vary between 15 and 22 A m^2/kg. As shown in the same figure, these calculations are in qualitatively good agreement with experimental results obtained in a previous work on a different single-crystalline sample of the same compound by Sinnema.[12]

The difference between our experimental results and Sinnema's experimental data can be ascribed to differences in stoichiometry in the samples used.[18] The small variations in stoichiometry lead to deviations in the crystal electric-field interaction in the compound (and hence in A_n^m). In this way differences must be found as well in the CEF parameters values depending on the particular sample studied. In Ho_2Fe_{17} variations in the crystal field lead to the fact that for some particular stoichiometries the easy magnetization direction can lie slightly away from the **b** axis. According to our calculations the iron and rare-earth sublattices are not perfectly antiparallel in Sinnema's sample, but present an angle

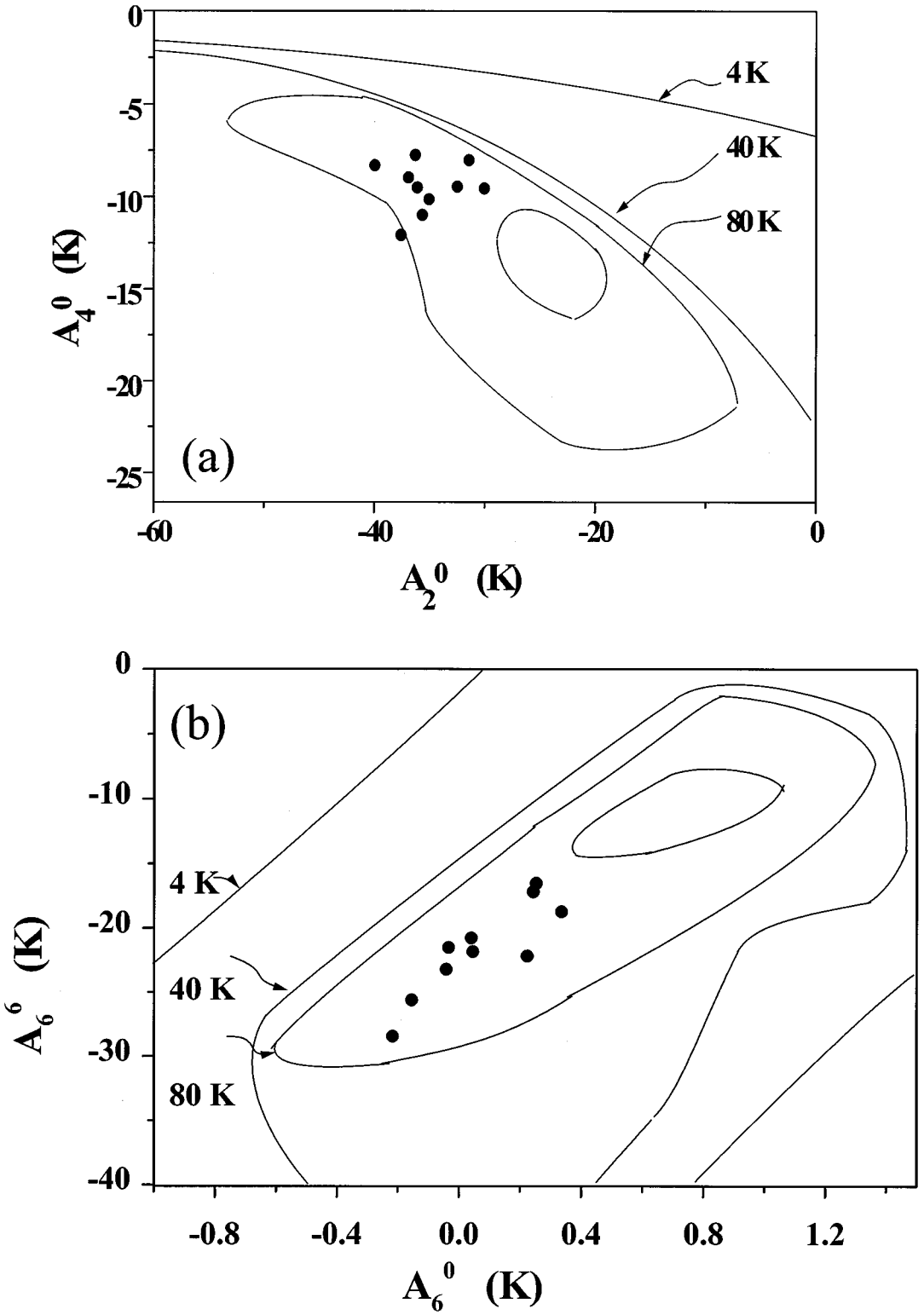

FIG. 10. Projection on the A_2^0/A_4^0 (a) and A_6^6/A_6^0 planes (b), of the $\{A_n^m\}$ parameter sets: the solid lines represent the same contours as in Figs. 5(a) and 5(b), in the process of parameter search for the erbium-based compound. The solid circles represent the solution determined for Dy_2Fe_{17} in this work (see text).

of about 179.1°, and the iron magnetization lies on the **bc** plane showing a small component along the **c** axis (θ=78.9°, approximately).

It is interesting to compare these results with the calculations given by a CEF parameter set giving an acceptable fit to our experimental results. As the experimental magnetization behavior is known in a wide temperature range for this compound, we are able to follow the same process described in Sec. IV A for determining, in this case, the CEF parameters in the holmium-based intermetallic. The resulting solution is shown in Figs. 14(a) and 14(b). In this figure the inserted squares correspond to the successive scans made for

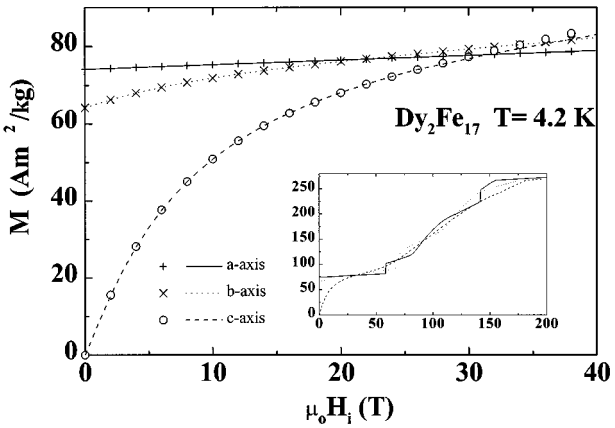

FIG. 11. Magnetization isotherms of Dy_2Fe_{17} for the field applied along the directions **a**, **b** and **c** at 4.2 K. The solid lines represent the calculation obtained using the parameter set determined in this work (see Table I), the symbols correspond to experimental results of Ref. 12. The inset shows the predicted calculation for higher-field values.

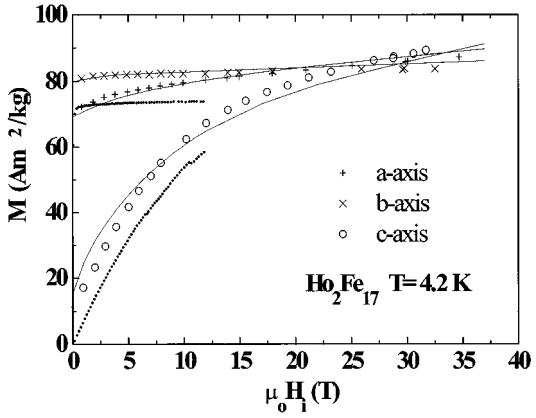

FIG. 13. Experimental and calculated magnetization isotherms for Ho_2Fe_{17} with the field applied along the different directions at 4.2 K. The symbols represent the data taken from Ref. 12 that can be compared with our measurements for the **b** and **c** directions on a different sample (dots). The lines correspond to the calculation using the parameters determined for Er_2Fe_{17} (see Table I).

reaching the final solution. A determination of the particular thermal variation of the $3d$-sublattice magnetization had to be performed for this compound, in order to explain the magnetic behavior observed at high temperatures. This dependence was calculated so that the predicted saturation magnetization agreed with the one observed in the high-temperature measurements. For that we selected different parameter sets giving a good fit to the measurements in the low-temperature range, in which the $3d$ magnetization varies very little. The thermal variation determined was observed to be practically independent of the selected set, and is shown in Fig. 1.

Between the solution sets found for Ho_2Fe_{17}, we have selected the parameters giving the best fit to the 4.2 K measurements. The values obtained are shown in Table I. The calculated magnetization is given together with our experimental results at 4.2 K in Figs. 15 and 16. The spontaneous magnetization lays in this case on the **b** axis, and the two

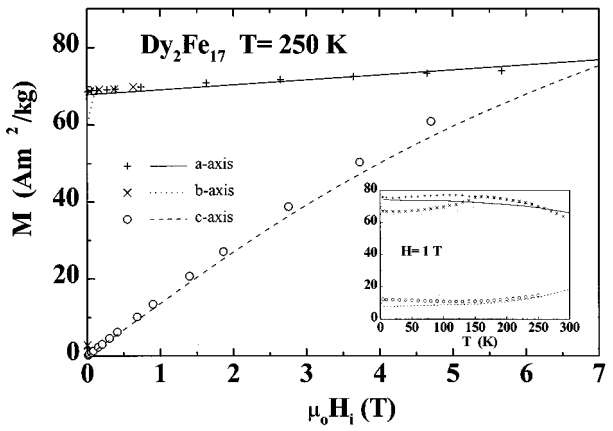

FIG. 12. Magnetization isotherms of Dy_2Fe_{17} for the field applied along the directions **a**, **b**, and **c** at 250 K. Insert: Temperature dependence of the magnetization for a field of 1 T applied along the directions **a**, **b**, and **c** for Dy_2Fe_{17}. The solid lines represent the calculation using the parameter set determined in this work (see Table I), the symbols correspond to experimental results of Ref. 12.

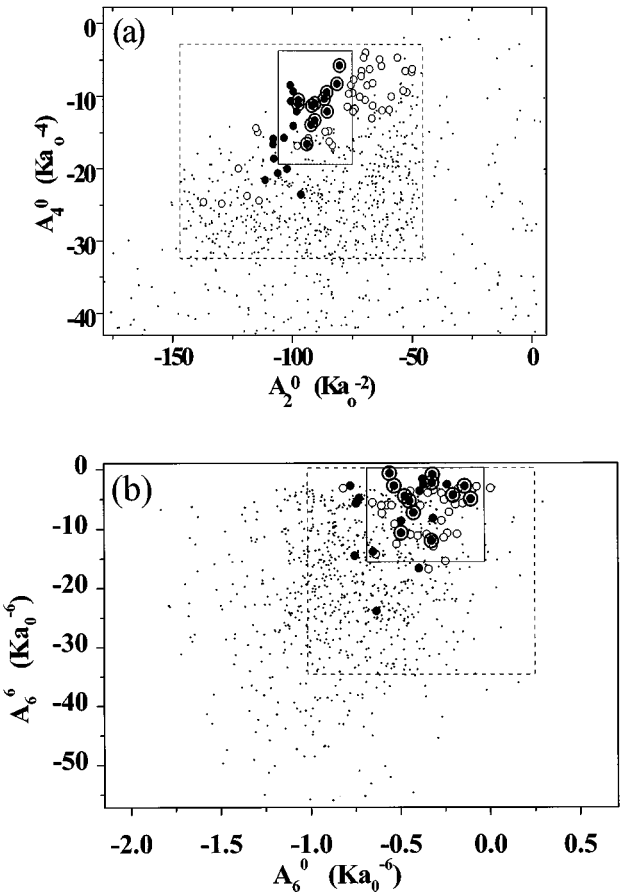

FIG. 14. Projection on the A_2^0/A_4^0 (a) and A_6^0/A_6^6 (b) planes, of the $\{A_n^m\}$ parameter sets. The four-dimensional solutions fitting the $T=4.2$ K **c** isotherm (dots), $T=100$ K (open circles), $T=150$ K (solid circles), and the sets fitting the whole temperature range isotherms (hollow big circles) for Ho_2Fe_{17}. The dashed line indicates the space parameter region that was deeply analyzed after previous scans.

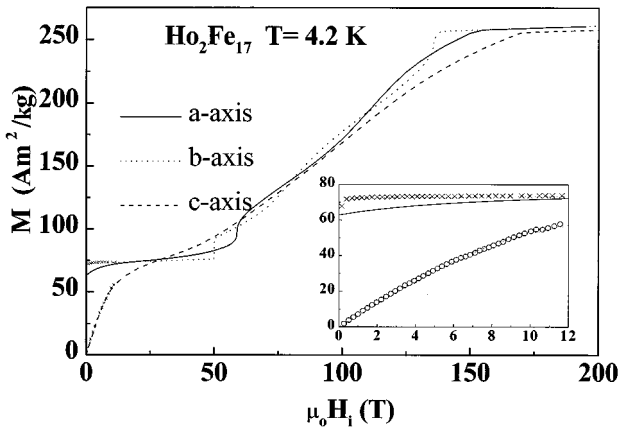

FIG. 15. Magnetization isotherms at 4.2 K for Ho_2Fe_{17}. The solid lines represent the calculation for the parameters determined for this compound (see Table I), the symbols correspond to our experimental results along the **b** and **c** directions, respectively. The inset shows the calculated and measured results for the low-field range.

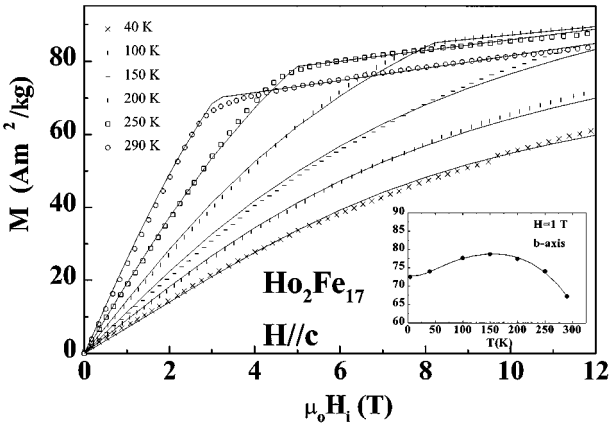

FIG. 16. Magnetization isotherms of Ho_2Fe_{17} for the field applied along the hard-**c** direction at different temperatures. Inset: temperature dependence of the magnetization for a field of 1 T applied along the **b** direction for Ho_2Fe_{17}. The solid lines represent the calculation for the set of parameters determined for this compound (see Table I), the symbols correspond to experimental results.

sublattices are perfectly antiparallel. The field-induced transitions are expected to take place at 63.9 T for the **a** axis, and at 52.2 T for the **b** axis. The two sublattices become parallel under applications of the field of the order of 200 T.

V. CONCLUSIONS

The CEF-parameter space has been analyzed systematically in order to determine the values describing the CEF interaction in some R_2Fe_{17} compounds. Experimental magnetization measurements on single crystals in a wide temperature range (from 4.2 to 300 K) have been used to contrast the results. A limited region in the parameter space is found for the solution describing the CEF interaction in the compounds Er_2Fe_{17}, Dy_2Fe_{17}, and Ho_2Fe_{17}. The solution region given for the different intermetallics is close when expressed in terms of the A_n^m CEF parameters, but no common set can be found for explaining the magnetization behavior of the three compounds. The magnetization has been calculated using the two-site averaged parameters giving the best fit for each compound. The results show satisfactory agreement with the experimental magnetization curves, as well as with the measured thermal variation of magnetization. The success of the calculations using an averaged CEF parameter set for $R=$Dy, Ho, and Er suggests that for these compounds the two rare-earth sites existing in the hexagonal crystallographic structure present qualitatively similar behaviors.

The averaged A_2^0 CEF parameters determined for Er_2Fe_{17} are in agreement with the results of the ^{166}Er Mössbauer effect in Er_2Fe_{17}, for which the range $A_2^0 \sim -50 \pm 100\ Ka_0^{-2}$ was found.[29] This value for the second-order CEF parameter is smaller than the one observed for Gd_2Fe_{17} with Th_2Zn_{17} structure, $A_2^0 = -351 Ka_0^{-2}$,[30] and for the Gd_2Co_{17}, $A_2^0 \sim -375 Ka_0^{-2}$ from ^{155}Gd Mössbauer spectroscopy.[31] The determined CEF parameter A_6^6 presents for all the compounds studied in this work a non-negligible value, in agreement with the experimental results and evidencing the limitations of the PCM (from which a negligible value is predicted).

The A_2^0 parameter is negative for all the studied compounds. Generalizing this result to the rest of the intermetallic in the series, the positive α_J ions (Sm^{3+}, Er^{3+}, Tm^{3+}, Yb^{3+}) give a uniaxial contribution to the magnetic anisotropy, competing with the planar contribution of the Fe sublattice. In fact, the first-order moment process observed experimentally in Tb_2Fe_{17},[32] and Tm_2Fe_{17},[4] is qualitatively explained using the parameters determined for Er_2Fe_{17}, although a refinement of the particular values has to be done for adjusting the position of the critical field at which the process takes place in each case. This refinement has not been carried out in the present work, due to the lack of enough experimental data to impose sufficient restrictions on the CEF parameters to arrive at a reliable solution.

*Author to whom correspondence should be addressed. FAX: (34) 76.761229. Electronic address: berta@posta.unizar.es

[1] J. M. D. Coey and H. Sun, J. Magn. Magn. Mater. **87**, L215 (1990).

[2] Motohiko Yamada, Hiroaki Kato, Hisao Yamamoto, and Yasuaki Nakagawa, Phys. Rev. B **38**, 620 (1988).

[3] Bo-Ping Hu, Hong-Shuo Li, and J. M. D. Coey, Phys. Rev. B **41**, 2221 (1990).

[4] A. V. Andreev, A. V. Dergayin, S. M. Zadvrokin, N. V. Kudrevatykh, V. N. Moskalev, R. Z. Levitin, Y. F. Popov, and R. Y. Yumaguchin, in *Fizika Magnitnykh Materialov (Physics of Magnetic Materials)*, edited by D. D. Nishin (Sverdlovsk State University, Russia, 1985), pp. 21–49 (in Russian).

[5] K. Clausen and B. Lebech, J. Phys. C. **15**, 5095 (1982).

[6] Xiu-Feng Han, Han-Min Jin, Yu Yan, C. C. Sun, and B. F. Li, Phys. Status Solidi B **171**, k35 (1992).

[7] Xiu-Feng Han, Han-Min Jin, T. S. Zhao, and C. C. Sun, J. Phys. Condens. Matter **5**, 8603 (1993).

[8] J. J. M. Franse and R. J. Radwańnski, in *Handbook of Magnetic Materials*, edited by K. H. J. Buschow (North-Holland, Amsterdam, 1993), Vol. 7.
[9] B. García-Landa, P. A. Algarabel, M. R. Ibarra, F. E. Kayzel, T. H. Ahn, and J. J. M. Franse, J. Magn. Magn. Mater. **140–144**, 1085 (1995).
[10] B. García-Landa, M. R. Ibarra, P. A. Algarabel, and O. Moze, Phys. Rev. B **51**, 15 132 (1995).
[11] K. Clausen and O. V. Nielsen, J. Magn. Magn. Mater. **23**, 237 (1981).
[12] S. Sinnema, Ph.D. thesis, University of Amsterdam, 1988.
[13] M. T. Averbuch-Pouchot, R. Chevalier, J. Deportes, B. Kebe, and R. Lemaire, J. Magn. Magn. Mater. **68**, 190 (1987).
[14] W. Sucksmith and J. E. Thompson, Proc. R. Soc. London Ser. A **225**, 362 (1954).
[15] H. P. Klein, A. Menth, and R. S. Perkins, Physica **80B**, 153 (1975).
[16] J. Deportes, B. Kebe, and R. Lemaire, J. Magn. Magn. Mater. **54–57**, 1089 (1986).
[17] D. Givord, R. Lemaire, J. M. Moreau, and E. Roudaut, J. Less Common Met. **29**, 361 (1972).
[18] R. Kumar and W. B. Yelon, J. Appl. Phys. **67**, 1 (1990).
[19] J. V. Florio, N. C. Baezingerand, and N. E. Rundle, Acta Crystallogr. **9**, 367 (1956).
[20] K. W. H. Stevens, Proc. Phys. Soc. London Sect. A **65**, 209 (1952).
[21] J. E. Greedan and V. U. S. Rao, J. Solid State Chem. **6**, 587 (1973).
[22] J. K. Yakintosh, Phys. Status Solidi B **82**, 349 (1977).
[23] P. C. M. Gubbens, A. M. van der Kraan, J. J. van Loef, and K. H. J. Buschow, J. Magn. Magn. Mater. **67**, 255 (1987).
[24] P. C. M. Gubbens, A. M. van der Kraan, and K. H. J. Buschow, J. Magn. Magn. Mater. **54–57**, 483 (1986).
[25] R. Coehoorn, K. H. J. Buschow, M. W. Dirken, and R. C. Thiel, Phys. Rev. B **42**, 4645 (1990).
[26] J. J. M. Franse, F. E. Kayzel, T. Inou, K. Sugiyama, A. Yagamashi, and T. H. Anh (unpublished).
[27] S. Sinnema, J. J. M. Franse, R. J. Radwanski, A. Menovsky, and F. R. de Boer, J. Phys. F **17**, 233 (1987).
[28] S. Sinnema, R. Verhoef, J. J. M. Franse, and F. R. de Boer (unpublished).
[29] P. C. M. Gubbens, A. A. Moolenaar, G. J. Boender, A. M. van der Kraan, T. H. Jacobs, and K. H. J. Buschow, J. Magn. Magn. Mater. **97**, 69 (1991).
[30] O. Isnard, P. Vulliet, A. Blaise, J. P. Sanchez, S. Miraglia, and D. Fruchart, J. Magn. Magn. Mater. **131**, 83 (1994).
[31] P. C. M. Gubbens, A. M. van der Kraan, and K. H. J. Buschow, J. Phys. (Paris) Colloq. **49**, C8-525 (1988).
[32] R. Verhoef, Ph.D. thesis, University of Amsterdam, 1990.